Remote Sensing of Environment 112 (2008) 3511–3519

Contents lists available at ScienceDirect

Remote Sensing of Environment

journal homepage: www.elsevier.com/locate/rse

A generalizable method for remote sensing of canopy nitrogen across a wide range of forest ecosystems

M.E. Martin [a,*], L.C. Plourde [b], S.V. Ollinger [b], M.-L. Smith [c], B.E. McNeil [d]

[a] Complex Systems Research Center, Univ of New Hampshire, Morse Hall, 39 College Road, Durham, NH 03824, United States
[b] University of New Hampshire, United States
[c] USDA Forest Service Northern Research Station, United States
[d] University of Wisconsin, United States

ARTICLE INFO

Article history:
Received 24 April 2007
Received in revised form 10 April 2008
Accepted 12 April 2008

Keywords:
Hyperspectral
AVIRIS
Hyperion
Foliar nitrogen
Remote sensing

ABSTRACT

A growing number of investigations have shown that remote sensing of foliar nitrogen (N) concentration in plant canopies can be achieved with imaging spectroscopy, or hyperspectral remote sensing, from satellite or airborne sensors. Development of this approach has been fueled by recognition that foliar N is related to a variety of ecological and biogeochemical processes, ranging from the spread of invasive species to the ecosystem effects of insect defoliation events to patterns of N cycling in forest soils. To date, most studies have focused on building site-specific foliar N detection algorithms applied to individual scenes or small landscapes that have been intensively characterized with local field measurements. However, the growing number of well-measured sites, combined with improvements in image data quality and processing methods provide an opportunity to begin seeking more general N detection methods that can be applied to a broader range of sites or to locations that lack intensive field measurements.

Here, we combine data from several independent efforts in North America, Central America and Australia, to examine whether development of calibration methods to determine canopy nitrogen concentration across a wide range of forest ecosystems is possible. The analysis included data from 137 individual field plots within eight study sites for which imagery has been acquired from NASA's Airborne Visible/Infrared Imaging Spectrometer (AVIRIS) and/or Hyperion instruments. The combined dataset was used to evaluate site-specific calibration results as well as results obtained with data pooled across all sites. We evaluated the accuracy of results using plot- and site-level cross-validation wherein individual plots or entire sites were withheld and used as an independent validation of the resulting algorithms. In instances where all sites were represented in the calibration, canopy-level foliar N concentration was predicted to within 7–15% of the mean field-measured values indicating a strong potential for broadly applied foliar N detection. When whole sites were iteratively dropped from the calibration and predicted by remaining data, predictions were still significant, but less accurate (7–47% of mean canopy-level N concentration). This suggests that further development to include a wider range of ecosystems will be necessary before cross-site prediction accuracy approaches that seen in site-specific calibrations. Nevertheless, we view these results as promising, particularly given the potential value of foliar N estimates, even at a reduced level of confidence, at sites for which there is no possibility of conducting field data collections.

1. Introduction

The mass-based concentration of nitrogen in foliage is a key feature of forest canopies that influences a variety of important ecosystem processes. Foliar nitrogen (N) concentration is a primary regulator of physiological processes such as photosynthesis and leaf respiration (Evans, 1989; Field & Mooney, 1986; Reich et al., 1998, 2006) and is related to canopy and stand-level traits such as light use efficiency, wood growth and net primary production (Green et al., 2003; Ollinger & Smith, 2005; Smith et al., 2002) and soil factors such as litter quality, decomposition and nutrient mineralization (Aber et al., 1990; Ollinger et al., 2002; Scott & Binkley, 1997). Spatial variation in foliar N is caused by a combination of local factors such as tree species composition, soil type and disturbance history (McNeil et al., 2005; Ollinger et al., 2002), and regional- to continental-scale factors such as latitude, mean annual temperature, nitrogen deposition and incident solar radiation (Haxeltine & Prentice, 1996; McNeil et al., 2005; Yin, 1992). Temporal variation can result from short-term changes in climate or disturbance, or longer-term processes such as N deposition or plant exposure to rising CO_2 (Magill et al., 2004; Nowak et al., 2004).

* Corresponding author.
E-mail address: mary.martin@unh.edu (M.E. Martin).

0034-4257/$ – see front matter © 2008 Elsevier Inc. All rights reserved.
doi:10.1016/j.rse.2008.04.008

Given the importance of foliar N in ecosystem processes and the complexity of predicting spatial patterns across a range of scales, it is not surprising that effort has been directed towards methods of detection using remote sensing. The ability to remotely sense foliar N was first demonstrated soon after the advent of airborne imaging spectrometers. Initial work in this field (Wessman et al., 1988) built upon a history of laboratory spectroscopy in the field of agriculture (Norris et al., 1996; Shenk et al., 1979; Williams et al., 1984), but marked a shift from analysis of individual dried-ground samples to multi-pixel analysis of fresh vegetation at the canopy level. During the past two decades imaging spectrometers that have been developed include the NASA Airborne Visible/Infrared Imaging Spectrometer (AVIRIS), the EO-1 Hyperion space-based instrument, and numerous airborne commercial instruments. Using both AVIRIS and Hyperion, investigators have recently been able to predict image-scale foliar chemistry based on intensive plot sampling (Asner et al., 2006; Coops et al., 2003; Martin & Aber, 1997; Ollinger et al., 2002; Smith et al., 2002, 2003; Townsend et al., 2003; Wessman et al., 1988) and through applications of advanced photon transport models that include relationships between leaf reflectance properties and biochemical constituents (Asner et al., 1998; Asner & Vitousek, 2005). In addition to these individual-site studies, the work of Kokaly and Clark (1999) has evaluated foliar nitrogen concentration with respect to dried-leaf reflectance over a wide range of species using a continuum-removal technique. Huang et al. (2004) has built upon this technique in their analysis of eucalypt tree-level reflectance spectra.

Despite the potential power of canopy N detection with hyperspectral remote sensing, the number of applications has been limited by data availability, difficulties associated with correcting for atmospheric effects and the expense of field campaigns required for image calibration for each individual scene. However, over the past 5–10 years, there have been substantial improvements both in sensor signal-to-noise ratios and methods for atmospheric correction. Over that same time period, the number of field sites where foliar chemistry data and coincident imagery have been collected has grown steadily. Subsequently, it is now possible to seek more generalized canopy chemistry algorithms that can be applied across a range of sites and remote sensing scenes. Development of a generalized and, hence, more operational approach would expand both the scientific user base and the ecological utility of the growing volumes of hyperspectral data that have become available. The focus of this paper is to describe an effort to combine multiple image datasets from a wide range of forest ecosystems in the development and validation of a canopy foliar nitrogen concentration algorithm that will not require image-specific plot data and calibration. In recent years, we have acquired image and plot data for multiple datasets covering diverse forested sites (mixed hardwood and conifer, tropical species), over a wide geographic range (from northern New England to Northern Florida, to Central America and Australia). These datasets have provided a unique opportunity to revisit the issue of developing a generalized foliar N prediction equation across a diversity of sites.

2. Methods

The analysis described in this paper was made possible through a combination of datasets collected from 2001 to the present. Prior to this effort, data were collected and analyzed for each site individually. With this effort, we combine data from eight different sites with consistent field data collections and image data from one of two hyperspectral instruments.

2.1. Study sites

Five of the eight sites in this study were sampled under a NASA-funded North American Carbon Program field and remote sensing campaign. The five sites, each centered on a carbon flux tower, represent a latitudinal gradient from lower coastal plain pine plantations in Florida through mixed northern hardwoods in Massachusetts and New Hampshire to the cool, moist spruce-dominated forests of Maine. Three additional study areas were sampled by this research team through different projects, and include data from New York State, Costa Rica, and Australia. The sites included in this analysis are as follows:

Austin Cary Memorial Forest (ACMF, Florida) 29.75° N, 82.20° W. This site comprises two AmeriFlux towers in slash pine–long-leaf pine stands (*Pinus palustris* P. Mill., *Pinus elliottii*. Engelm.). Maintained by the University of Florida, the ACMF houses a flux tower in a 65-year-old naturally regenerated slash pine–long-leaf pine forest. A tower in the adjacent Donaldson Tract measures CO_2 flux in a long-leaf pine plantation that has been regenerating since 1990 (Gholz & Clark, 2002).

Duke Forest (DF, North Carolina) 35.97° N, 79.09° W. Two of three flux towers operated in the Duke University-owned Duke Forest are included at this study site: one in an even-aged loblolly pine (*Pinus taeda* L.) plantation (~17 years old), and the other in a mature mixed hardwood stand. Both are part of the AmeriFlux network (Oren et al., 2006).

Harvard Forest (HF, Massachusetts) 42.54° N, 72.17° W. The Harvard Forest site includes native mixed hardwood and conifer stands and a series of conifer plantations, mainly derived from old agricultural fields and pastures. The site was established in 1907 by Harvard University, and is one of 24 NSF Long-Term Ecological Research sites. Data from the Harvard Forest includes the longest continuous carbon balance record for a forest ecosystem (Goulden et al., 1996; Wofsy et al., 1993).

Bartlett Experimental Forest (BEF, New Hampshire) 44.06° N, 71.29° W. The USDA Forest Service-administered Bartlett Experimental Forest is a 1050-hectare tract of secondary successional northern hardwood and mixed northern conifer forest located in the central White Mountain region of New Hampshire (Ollinger & Smith, 2005). In the early 1930s the USDA Forest Service Northeastern Research Station established 500 permanent (0.1 ha) plots across the BEF. The majority of these plots (444) have been re-measured in at least three periods, the most recent being in 2002. Elevations range from 200 m to more than 850 m. In 2003, an eddy covariance tower was constructed at Bartlett, and has been in continuous operation since April 2004 (Jenkins et al., 2007). This tower is part of the AmeriFlux network and is a North American Carbon Program Tier III site.

Howland Forest (HOW, Maine) 45.20° N, 68.74° W. The Howland Forest is located in the boreal-northern hardwood transitional zone and consists of stands dominated by spruce, hemlock, and other conifer species. Flux measurements were initiated in 1995 and there are now three ~30-m-tall flux towers located in structurally and floristically similar stands. One of these continues to be operated as a control treatment while ecosystem-scale manipulations (i.e. nitrogen fertilization, harvesting) have been initiated around the other two towers. All three towers are part of the AmeriFlux network (Hollinger et al., 1999).

Adirondack Park (AP, New York) 44.00° N, 74.40° W. The largely forested expanses of the Adirondack Park cover a mountainous landscape ranging from 300 to 1500 m in elevation. Northern hardwood forests grade into the boreal forests that occur above 750 m in elevation or within poorly-drained valley bottoms. Over half of the Adirondack Park's 2.5 million hectares are preserved by New York State as “forever wild”, while the remaining half are privately owned and managed as conservation easements, logging tracts, or commercial and residential land within small towns and villages. Field plots were drawn from a wide variety of forest alliances (McNeil, 2006) and located within a subset of watersheds that have been studied for surface water chemistry by the Adirondack Long Term Monitoring program (Driscoll et al., 2003) or the Direct Delayed Response Program (Lee et al., 1989).

La Selva (LS, Costa Rica) 10.42° N, 84.02° W. A humid tropical rain forest in the Caribbean lowlands of northern Costa Rica, the La Selva Biological Station resides on land with a rich land-use history that includes shifting cultivation, selective cutting, and some clearing for

pasture. Originally established in 1954 as an experimental farm of mixed plantations for the purpose of studying natural resources management, it was purchased in 1968 by the Organization for Tropical Studies as a private biological reserve station. La Selva today comprises 1600 ha of primary and secondary tropical forest and has become one of the leading sites in the world for research on tropical rain forests. Foliage was sampled in 2006 by plant functional type (Loescher et al., 2003).

Bago-Maragle State Forest (BAGO, Australia) 35.75° S, 148.25° E. Located in southern New South Wales, Australia, the BAGO site is located in a cool to cold moist subalpine climate. The topography of this 50,000 ha study area ranges from a gently undulating plateau to deeply incised valleys and escarpment, with an elevational range of 400 to 1438 m. The plots sampled covered the full range of eucalypt species present, and were sampled in February 2001 to correspond to a hyperspectral data acquisition in support of NASA's EO-1 Science Validation Team (Coops et al., 2003).

2.2. Field data collection and analysis

At each research site, field data were collected for 14–25 plots. Sampling included the collection of fresh foliage for nitrogen analysis, and characterization of foliar biomass distribution by species through an optical point-quadrat method (Smith & Martin, 2001). Plots were typically 20×20 m in size, with slight variations due to initial plot establishment history. Although field and image acquisitions were not always in the same year, field collections were made in the peak of the growing season, and corresponding image data were selected on the basis of availability and to best match the seasonality of field collections. The suite of field data collections were combined to generate a plot-level or "whole canopy" estimate of foliar nitrogen concentration.

On each plot, at least 3 trees of each dominant overstory species were sampled. Leaves were collected by shooting small branches from the canopy with a shotgun, with each sample consisting of leaves composited from several heights in the canopy. For needle-leaved species, samples were a composite of all needle age-classes. The samples were oven dried at 70 °C and ground with a Wiley Mill to pass through a 1 mm mesh screen. For all sites except the Adirondack Park, analysis for foliar nitrogen concentration was done on a FOSS NIR 6500 spectrometer, for which a calibration relating spectral absorbance to traditional nitrogen chemistry has been developed (Bolster et al., 1996). For the Adirondack Park samples, analysis for foliar N concentration was conducted using the traditional CHN combustion technique.

Species fraction of canopy biomass was determined by the use of a camera point-quadrat sampling combined with leaf mass per area (LMA) measurements. The camera point-quadrat method has been demonstrated to be an accurate means of determining the relative distribution or fraction of leaf area by height in a forested canopy (Aber, 1979a,b; Smith & Martin, 2001). In each field plot, 15 grid point observations at nine sampling stations were taken (plot center and each of the four cardinal and off-cardinal directions at 15 m from plot center) for a total of 135 observations per plot. The sampling device was a 35-mm camera with a telephoto lens used as a range finder (calibrated to distance in meters) and a 15 point gridded focusing screen. Fraction of leaf *area* by height and by species were determined with this method, and conversion to fraction of species by leaf *weight* was made with LMA data. LMA data sources varied by site, with some site/species-specific measurements available. When site/species-specific data were not available, LMA data as reported in the literature were used (Reich et al., 1999; Smith & Martin, 2001; Wright et al., 2004). A comparison of the camera-based method and the more conventional litterfall mass-based calculations of canopy-level nitrogen concentration demonstrated nearly identical prediction of mass-based nitrogen concentration among sample plots (Smith & Martin, 2001).

Plot-level foliar nitrogen concentration was calculated as the mean foliar nitrogen concentration for each species, weighted by species canopy mass fraction. The distribution of canopy nitrogen concentration measured at each site is shown in Fig. 1.

2.3. Hyperspectral data

2.3.1. Data collection

Hyperspectral data were obtained in 2001–2006 for eight sites in the eastern U.S., Costa Rica, and Australia (Table 1). NASA's Airborne Visible/Infrared Imaging Spectrometer (AVIRIS) was flown on the ER-2 platform and collected data in an 11 km swath over Duke Forest, North Carolina and Austin Cary Memorial Forest, Florida, in 2002, and over Howland Forest, Maine, Bartlett Experimental Forest, New Hampshire, and Harvard Forest, Massachusetts in 2003. The AVIRIS sensor captures upwelling spectral radiance in 224 contiguous spectral bands for wavelengths from 400 to 2500 nm, with a 10 nm nominal bandwidth. The ER-2 flies at approximately 20 km above sea level, resulting in a pixel size of approximately 17 m.

Hyperspectral data were collected over the same AVIRIS sites by NASA's spaceborne Hyperion sensor between 2002 and 2005. In addition, Hyperion imagery was collected over the Adirondacks region of New York, the La Selva Biological Station, and the Bago-Maragle State Forest in NSW, Australia (2001–2006). Mounted on the EO-1 satellite (Pearlman et al., 2003), Hyperion orbits the earth at 705 km above sea level, and records radiance in 220 bands with the same

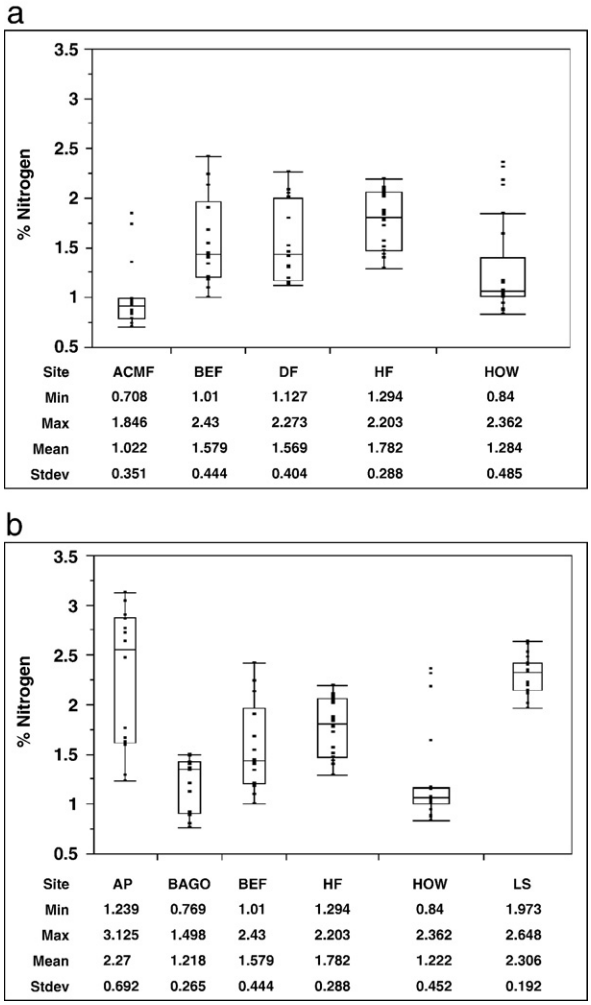

Fig. 1. Plot-level foliar N distribution from field measurements across all sites. a) Sites included in AVIRIS analysis. b) Sites covered in Hyperion analysis.

Table 1
Dates of field and image data collection

	Image data		
	AVIRIS	Hyperion	Field data (number of plots)
DF	May 2002	–	June 2002 (16)
ACMF	June 2002	–	June 2002 (15)
HF	August 2003	September 2002	July 2002 (20)
HOW	August 2003	August 2002	July 2002–03 (25,23)[a]
BEF	August 2003	August 2002	Jul–Aug 2005 (14)
AP	–	September 2003	Jul–Aug 2003 (14)
LS	–	February 2006	Mar–Apr 2006 (19)
BAGO	–	April 2001	Feb 2001 (14)

[a] Number of plots used for Howland site varies between AVIRIS and Hyperion analysis due to slightly different geographic coverage.

spectral range as AVIRIS, 10 nm spectral resolution, and 30 m spatial resolution, for a 7.7 km swath. Although the signal-to-noise ratio for Hyperion data is lower than that of AVIRIS, it is more widely available at the current time, and provides an opportunity to demonstrate the potential capabilities for space-based hyperspectral data in this application.

We conducted two parallel analyses for AVIRIS and Hyperion data, when possible. However, data were not available for all eight sites for both instruments; AVIRIS data were available for only five of the U.S. sites, and suitable Hyperion were available for only six of the eight sites. At ACMF and DF, the available Hyperion data had been acquired after leaf senescence, eliminating those sites from inclusion in this analysis. The image data used in this paper were limited to those data collected during a similar phenological period as the field data; typically within a 1–2 month phenological window of the corresponding field data collection.

2.3.2. Preprocessing

Both AVIRIS and Hyperion were preprocessed using ENVI v.4.2 and ERDAS Imagine v.8.7. Image data were received as calibrated at-sensor radiance, and an initial band subsetting process removed uncalibrated bands from the Hyperion image data, and removed overlapping bands and those with low signal-to-noise ratios (e.g. water absorption bands) from both Hyperion and AVIRIS datasets. Image data were standardized by normalizing the mean and standard deviation of each column to the overall mean and standard deviation for each wavelength in the images. The main purpose of this standardization was to minimize a striping artifact present in Hyperion data (Datt et al., 2003), but it also minimized a view-angle brightness gradient apparent in some AVIRIS scenes. All image datasets were atmospherically corrected with ImSpec LLC's Atmospheric COrrection Now (ACORN) v.5.1, transforming data from calibrated sensor radiance to apparent surface reflectance. ACORN mode 1.5 was used for AVIRIS data ("Advanced atmospheric correction of hyperspectral data with spectral fitting for water vapor and vegetation liquid water"), and mode 1.5pb for Hyperion (the same as mode 1.5, but designed for pushbroom instruments with cross-track spectral calibration variation). Finally, all images were georegistered to known coordinates collected from USGS digital orthophotos and field GPS data.

2.4. Regression

While many fewer bands may provide the necessary signal to detect foliar N (e.g. Townsend et al., 2003), we chose to retain for regression analysis nearly the full-spectral range of each sensor in order to capture spectral information that may relate to foliar N in some currently undescribed manner. After removing bands that contained no data or that were visibly noisy, remaining bands were within the spectral regions of 400–1300 nm, 1400–1800 nm, and 2000–2500 nm (189 AVIRIS bands and 113 Hyperion bands at 10 nm bandwidth).

Reflectance spectra were extracted from the four pixels in the AVIRIS and Hyperion images nearest the coordinates for each field-measured N plot at each site, and averaged (a single exception was in the AP dataset, where the single nearest pixel was used). Partial least squares (PLS) regression was then used to relate these spectra to field-measured N (Ollinger & Smith, 2005; Smith et al., 2002, 2003). PLS regression is a type of eigenvector analysis that reduces the full spectrum to a smaller set of independent factors, with corresponding field data used directly during the spectral decomposition process (Kramer, 1998). Spectra were analyzed with PLS individually for each site, as well as together in a multi-site dataset. All PLS models were validated using a standard "leave-one-out" cross-validation, with the final model developed using all samples within a particular dataset. The calibration dataset compiled for this study incorporated more than 1000 individual foliage samples, representing more than 70 species collected from 137 plots among the study sites. For the AVIRIS and Hyperion analyses, image data were available for 90 and 104 field plots, respectively.

Three approaches were used in the evaluation of field and image data for the development of predictive canopy foliar nitrogen concentration equations. In each of the following cases, data from AVIRIS and Hyperion were analyzed separately:

1. A single calibration was developed for each site based on the field data available at that specific site. This method represents the technique used to date in hyperspectral studies of foliar chemistry (Coops et al., 2003; Smith et al., 2002, 2003; Townsend et al., 2003).
2. For each instrument, all data were combined into a single calibration file for the development of a multi-site calibration. In this approach, all plots from all sites were included, representing the full range of variability in both spectral and field conditions. In this first and second approach, the accuracy of the PLS equations developed is represented by the coefficient of determination (*R*-squared), while precision is determined by standard errors of performance. These include the standard error of calibration (SEC), a measure of the average difference between predicted and measured N at the calibration stage, and the standard error of cross-validation (SECV), which is the root mean square of the residuals derived from an iterative exclusion and prediction method, whereby a single data point (*plot*) is iteratively held back from the calibration and is predicted by the resulting calibration (Mark & Workman, 1991).
3. In the final approach, each *site* was iteratively excluded from a multi-site calibration which was then used to independently predict foliar N values for all plots within the excluded site. This approach evaluates the ability of the calibration technique to predict canopy foliar nitrogen concentration for sites which were not represented in any manner within the calibration dataset. In this final approach, SEP was calculated for plots within each individual site, to determine the ability of this technique to predict chemistry for entirely independent sites.

3. Results and discussion

3.1. Individual-site calibration

PLS regressions for each of the individual study sites demonstrated strong predictive relationships between spectral reflectance and whole canopy foliar N concentration, with R^2 values ranging from 0.69 to 0.85 for AVIRIS spectra, and from 0.45 to 0.83 for Hyperion spectra (SECV ranging from 0.13–0.23 and 0.16–0.32, respectively; Table 2, Fig. 2a). At the two ends of calibration performance, BEF and AP had the highest SECV, with the lowest SECVs at BAGO and LS. The higher SECV values at BEF and AP may be attributable to the wide variation in forest functional types (i.e. broadleaf deciduous vs. needle-leaf evergreen) within the BEF and AP sites. This forest type variation results in wide variation in both spectral reflectance and foliar N concentration at a local scale. The ACMF, BAGO, and LS sites had the lowest SECV, possibly due to the fact that

Table 2
Results from PLS regression of spectral response to whole canopy foliar N

Dataset	Plot-based cross-validation			Site-based cross-validation		
	R^2	SEC	SECV	R^2	SEP of predicted site	Bias
AVIRIS						
DF	0.81	0.14	0.17	0.84	0.16	−0.06
ACMF	0.85	0.09	0.13	0.81	0.26	0.21
HF	0.69	0.16	0.17	0.75	0.17	−0.02
HOW	0.79	0.17	0.22	0.81	0.17	0.05
BEF	0.73	0.20	0.23	0.81	0.25	0.05
All sites combined	0.83	0.18	0.19			
Hyperion						
BAGO	0.60	0.04	0.16	0.08	0.56	−0.50
BEF	0.63	0.24	0.26	0.75	0.25	0.10
HF	0.69	0.09	0.17	0.67	0.43	0.39
HOW	0.83	0.14	0.18	0.89	0.35	0.28
LS	0.45	0.14	0.16	0.38	0.17	0.05
AP	0.78	0.25	0.32	0.79	0.61	−0.53
All sites in multi-site equation	0.82	0.22	0.25			

Statistics reported for *plot-based cross-validation* represent measures of accuracy and precision for regression methods 1 (individual-site calibrations) and 2 (comprehensive multi-site site calibrations) described in the Methods. Statistics for *site-based cross-validation* represent performance of regression method 3, in which the site-by-site cross-calibration regression models were used to predict foliar N for independent sites not represented within the calibration dataset. SEC = Standard error of calibration (average difference between predicted and measured N), SECV = standard error of cross-validation (RMS of residuals derived from iterative *plot* exclusion and prediction), SEP of predicted site = standard error of cross-validation derived from iterative *site* exclusion and prediction, bias = systematic difference between predicted and measured values (average value of residuals) (Mark & Workman, 1991).

these respective sites are dominated by plants of a similar functional type. These two extremes (diverse vs. uniform functional plant types within a single site) correspond to the extremes in calibration performance. These functional and structural differences in leaf type and habit may also be related to differences in canopy structure in ways that modify the relationship between reflectance and foliar N. Despite differences in absolute model performance across sites, it is noteworthy that the SECV values across all sites fell within approximately 7 to 17% of their respective mean foliar N concentration values.

3.2. Comprehensive multi-site calibration

When reflectance spectra and corresponding measured canopy N were combined into a single dataset for each instrument (multi-site calibration; see regression approach 2 in Methods section), the positive linear relationship remained, with a slightly better calibration resulting from the multi-site AVIRIS dataset than the Hyperion dataset (*R*-squared 0.83 and 0.82, SECV 0.19 and 0.25, respectively; Table 2, Fig. 2b). This methodology has been published in a number of previous papers for individual sites, and both SECV and relative performance of the two instruments observed here are comparable with prior published results (Coops et al., 2003; Smith et al., 2003; Townsend et al., 2003).

3.3. Site-by-site Cross cross-calibration

As each site was iteratively excluded from the calibration (regression approach 3), results differed between sensors and among sites. In general, AVIRIS calibrations were better able to predict excluded sites than were Hyperion calibrations (Fig. 2c). The highest SECV for predicted foliar N resulted from independent predictions at the AP and BAGO sites (Table 2) — these sites represent plots at the high and low extremes of measured foliar N concentrations, respectively (Fig. 1). In the case of the AP site, plot-level N for several plots exceeds values found in any other site, and are therefore not represented in the calibration (Fig. 1). In this case, where we attempt to predict foliar N beyond the upper limit of the calibration dataset, we would expect the observed under-prediction for these sites. In addition to the difference in foliar N composition at this site, it is one of two sites where image data were acquired in September. It is possible that by mid-September, the imagery was collected at the onset of nitrogen retranslocation, and reflects an actual reduction of nitrogen concentration from that measured during the field data campaign.

At the Australian BAGO site — where the lowest foliar N values were observed — foliar N concentration was also consistently under-predicted. A possible explanation for this poor prediction is that by excluding these low foliar N values from the calibration, the canopy characteristics found at BAGO were not adequately represented by the balance of sites in this particular calibration model (similarly low foliar N values in this equation were found only in red spruce trees at the Howland, Maine site). Yet, when the BAGO site was included in the comprehensive multi-site calibration, the resulting equation performed well at sites with broad inter-specific variability of mixed functional type forests (e.g. Adirondack Park), as well as at sites characterized by the narrow range of foliar N and spectral variability which occurs within a single-genus forest. The independent predictions made for the LS plots resulted in the lowest R^2 of all sites. This may be due to the fact that this is the only tropical site in the study, and it is possible that although similar in canopy nitrogen to other sites, there may be canopy-level differences which are not represented in the balance of the study sites.

3.4. Relative importance of spectral bands in PLS calibrations

The relative influence of spectral regions on the determination of foliar N concentration was evaluated by weighting calibration equation coefficients with average spectral reflectance (Fig. 3). This method of evaluation compensates for those areas where coefficients may be large, but reflectance low, thereby reducing the influence of the large coefficient on predicted N. Results shown in Fig. 3 indicate a high degree of variation in the wavelength importance, with two important trends emerging. First, the most consistently influential reflectance channels occur in the NIR plateau, from 700–1250 nm, with a positive relationship between reflectance and foliar N throughout the region, and localized peaks at 817*, 922, 1107, 1192*nm (AVIRIS) and 762, 813*, 984*, 1225*nm (Hyperion). Wavelengths denoted with (*) have been described in the literature as spectral regions associated with the absorption of nitrogen compounds (Curran, 1989; Burns & Ciurczak, 1992; Osborne & Fearn, 1986; Williams, 2001). Specifically, these wavelengths have been associated with overtones and combination bands related to N–H and C–H bonds found in proteins. It is not surprising that other regions, not normally associated with nitrogen compounds, are also heavily weighted in the calibrations; these are likely associated with leaf compounds and/or leaf traits which co-occur with nitrogen compounds. Although the NIR plateau is also strongly influenced by water content and canopy structure, it can be noted that in the spectra of fresh leaves, reflectance in this region (800–1200 nm) is also highly correlated with nitrogen concentration (unpublished data). Secondly, a negative relationship is seen between foliar N and reflectance in the region of 720–730 nm. This negative relationship is expected in this chlorophyll absorption region, as increasing chlorophyll and nitrogen result in a decrease in reflectance. In the longer wavelength region of the NIR the influence of reflectance on the determination of foliar N is much lower, with localized peaks at 1730* and 2280* (AVIRIS), and 1497* and 2173* (Hyperion).

The relative importance of each band differs among AVIRIS and Hyperion datasets (Fig. 3), due to the fact that the available bands for each instrument differs. The bands eliminated from the analysis include those with low signal-to-noise, regions of strong atmospheric water absorption, and a number of uncalibrated Hyperion bands. Fig. 4 shows the weightings for the individual-site calibrations in the spectral regions discussed above, where AVIRIS and Hyperion datasets overlap (690–1090 nm). This figure shows that the relative importance

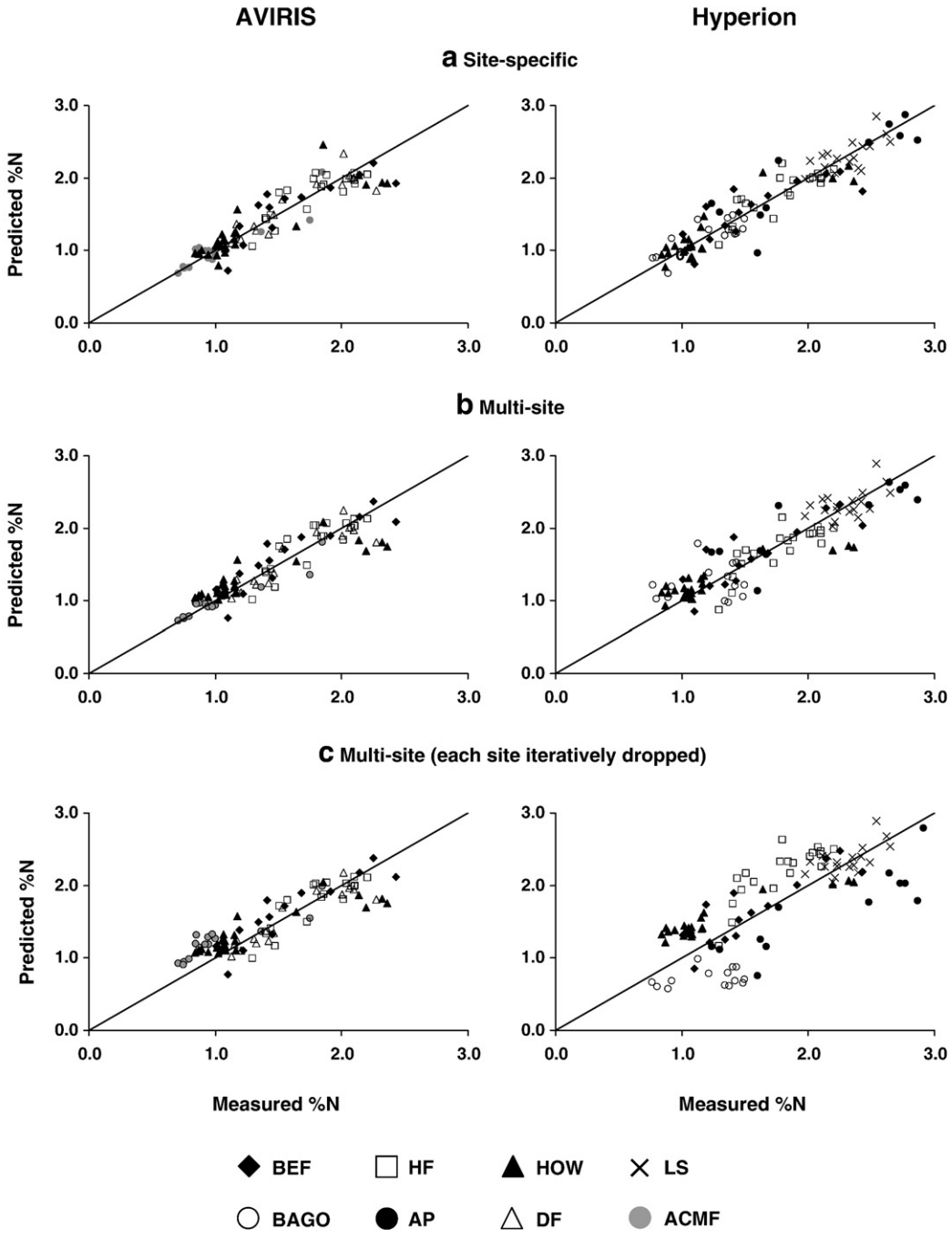

Fig. 2. Plot-level nitrogen concentration as measured in the field and predicted with AVIRIS and Hyperion data. a) Site-specific calibration, b) multi-site calibration, and c) multi-site calibration with site-level cross-validation.

of the reflectance spectra for determining canopy N concentration is consistent among the study sites.

3.5. Calibration considerations imposed by sites, instrument characteristics, and image processing methods

There are a number of important considerations in the current and future development of this generalized canopy foliar nitrogen prediction method, due to the multi-site, multi-image nature of this approach. Of particular importance are the methods used by individual investigators when compiling data from a variety of sources, ranging from field measurements to image sources and image processing techniques. We have limited this specific analysis to sites and imagery sampled and processed by the authors. As additional datasets are incorporated into this approach (sites, image data sources, etc.), it will be important to address a number of issues that have surfaced in this analysis.

As with any multi-scene, multi-date analysis, the conversion of at-sensor radiance to surface reflectance is extremely important. There are a number of software options for making this conversion, and an analysis of combined scenes will likely require application of a single correction method across the full suite of data. Although all methods may produce reasonable reflectance spectra (Kruse, 2004), subtle differences in output may make multi-scene analysis difficult.

Calibrations developed from AVIRIS data were consistently stronger than those from Hyperion, likely due to a combination of Hyperion's

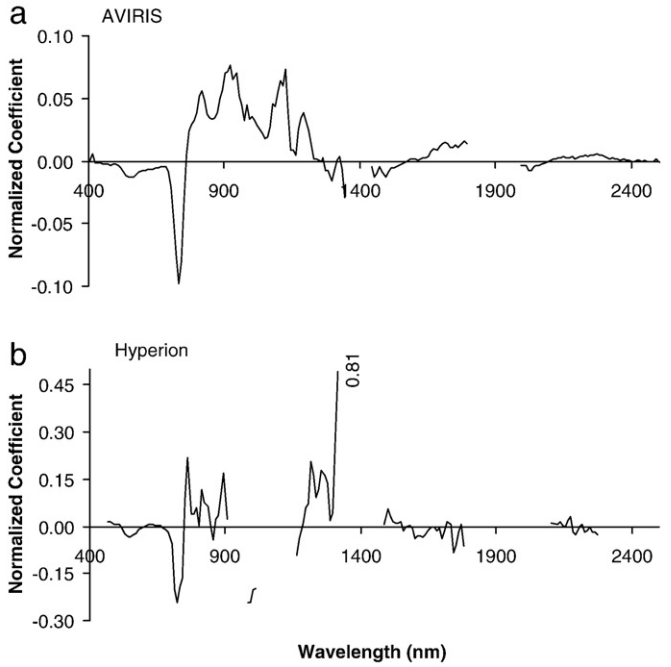

Fig. 3. Multi-site calibration equation coefficients normalized by average spectral reflectance for a) AVIRIS, and b) Hyperion. Single value noted on graph reflects an extreme value at 1326 nm.

coarser spatial resolution and much lower signal-to-noise ratio (SNR), which can be nearly an order of magnitude lower than AVIRIS SNR (Green, 2005; Kruse, 2003). In addition to the two instruments used in this paper, a number of commercial hyperspectral data acquisition options exist at the present time. However, before relying on foliar N predictions from these data sources, it will be important to carefully evaluate these data sources on the basis of spatial/spectral resolution and data quality. In the current work, we have not attempted to merge data from multiple instruments, nor have we transferred equations developed for one, to the other.

While previous work relating image data to foliar chemistry has often involved spectral smoothing with absorption or first-derivative transformation (e.g. Smith et al., 2003; Townsend et al., 2003) or continuum removal (Curran et al., 2001; Huang et al., 2004; Kokaly & Clark, 1999), foliar N calibrations with "unsmoothed" AVIRIS and Hyperion reflectance spectra in this study were slightly more robust than those with absorbance or first-derivative transformations. A possible explanation for this result is that the field sites captured in both AVIRIS and Hyperion scenes were near nadir, with an estimated sensor look angle ranging from less than 1° to 7° off-nadir. Further, with cross-track scanning and north–south orientation, neither AVIRIS nor Hyperion sensors were ever directly forelit or backlit. Finally, the PLS regression reduces full-spectrum data to a smaller set of factors; hence, the calibration itself minimizes bi-directional reflectance factors that may be present in reflectance spectra. Calibrating with reflectance data may also have the benefit of minimizing data loss caused by transforming or smoothing the data, thereby retaining the high information content available with hyperspectral imagery. As the development of a generalized canopy foliar nitrogen calibration continues, and site and image variability expand, it may be beneficial to address some of these other techniques.

Finally, with the exception of the slashpine plantation at the ACMF, the sites in this study represent closed canopy forests. Without representation of functional types found in shrublands, grasslands, or semi-arid systems, for example, some loss of prediction accuracy would be expected in these sites. Hence, new image and field data from a more diverse range of biomes would expand the applicability of a generalized model.

4. Conclusions

This study has shown that a generalized calibration developed from a combination of data from diverse study sites over multiple scenes can predict foliar N concentration at new sites. Images derived from the multi-site calibration are virtually identical in appearance to those derived from site-specific calibrations estimates, which are shown in other papers. For example, previous papers have used canopy nitrogen concentration images to predict patterns of forest productivity (Smith et al., 2002; Ollinger and Smith, 2005), and measures of soil N cycling (Ollinger et al., 2002) at the BEF site. McNeil (2006) developed a foliar N map from Hyperion data, which was then used in an analysis of the spatial controls on foliar N concentration within the Adirondack Park, NY (McNeil et al., 2005).

As this analysis progressed through the three methods (ranging from the inclusion of comprehensive field data for each site, to no field data), the ability to determine foliar N was reduced. However, the ability to apply a multi-site calibration model with even a reduced level of confidence opens up an enormous potential for sites that have hyperspectral coverage, but inadequate density of field data for site-specific calibration. The equation could be applied to virtually all image data collected and then validated against the existing field data. As new image and field data become available from more geographically and floristically diverse sites, and from a wider array of forest biomes, we

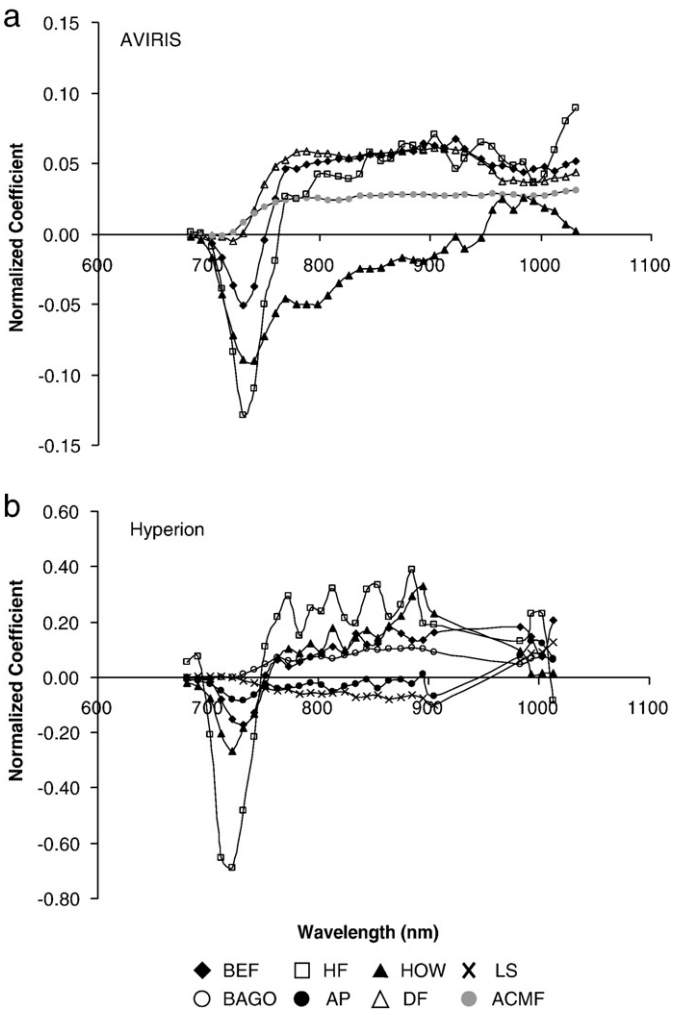

Fig. 4. Calibration equation coefficients normalized by average spectral reflectance by site for wavelengths from 690 nm to 1090 nm (a. AVIRIS, b. Hyperion). Note the consistency across sites in importance of weightings in the chlorophyll absorption area (~690–730 nm) and the NIR plateau (~750–1090 nm).

anticipate that this broader dataset will allow better characterization of "new" or less well-studied sites. Extending the prediction of canopy foliar nitrogen to these sites could greatly expand the number of possible foliar N applications. We suggest that some loss of prediction accuracy may occur when multiple plant functional types are included or when a particular functional group is not represented in the calibration model (e.g. Bago was poor when eucalypts were not included). It follows from this that efforts to improve detection of tree species and plant functional types would be a very useful complement to future improvements in foliar N detection.

Acknowledgments

AVIRIS and Hyperion data were collected by NASA, and provided to the authors in support of the following grants: NASA Carbon Cycle Science Program (CARBON/04-0120-0011), NSF Biocomplexity in the Environment (0421178), and EO-1 Science Validation Team (NCC5-477) and the W.M. Keck Foundation. Field data support was provided through the DOE National Institute of Global Environmental Change, the Hubbard Brook and Harvard Forest LTER Programs, the Bartlett Experimental Forest, and CSIRO.

References

Aber, J. D. (1979a). A method for measuring foliage-height profiles in broad-leaved forests. *Journal of Ecology*, *67*, 35–40.

Aber, J. D. (1979b). Foliage-height profiles and succession in northern hardwood forests. *Ecology*, *60*, 18–23.

Aber, J. D., Melillo, J. M., & McClaugherty, C. A. (1990). Predicting long-term patterns of mass-loss, nitrogen dynamics and soil organic matter formation from initial litter chemistry in forest ecosystems. *Canadian Journal of Botany*, *68*(12), 2201–2208.

Asner, G., Bateson, C., Privette, J., & El Saleous, N. (1998). Vegetation structural effects on carbon uptake using satellite data fusion and inverse modeling. *Journal of Geophysical Research*, *103*, 28839–28853.

Asner, G., Martin, R., Carlson, K., Rascher, U., & Vitousek, P. (2006). Vegetation–climate interactions among native and invasive species in Hawaiian rainforest. *Ecosystems*, *9*(1), 1106–1117.

Asner, G., & Vitousek, P. (2005). Remote analysis of biological invasion and biogeochemical change. *Proceedings of the National Academy of Sciences*, *102*, 4383–4386.

Bolster, K. L., Martin, M. E., & Aber, J. D. (1996). Interactions between precision and generality in the development of calibrations for the determination of carbon fraction and nitrogen concentration in foliage by near infrared reflectance. *Canadian Journal of Forest Research*, *26*, 590–600.

Burns, D. A., & Ciurczak, E. W. (1992). *Handbook of near-infrared analysis.* New York, NY, USA: Marcel Dekker.

Coops, N. C., Smith, M. L., Martin, M. E., & Ollinger, S. V. (2003). Prediction of eucalypt foliage nitrogen content from satellite-derived hyperspectral data. *IEEE Transactions on Geosciences and Remote Sensing*, *41*(6), 1338–1346.

Curran, P. J. (1989). Remote sensing of foliar chemistry. *Remote Sensing of Environment*, *30*, 271–278.

Curran, P. J., Dungan, J. L., & Peterson, D. L. (2001). Estimating the foliar biochemical concentration of leaves with reflectance spectrometry — Testing the Kolaly and Clark methodologies. *Remote Sensing of Environment*, *76*, 349–359.

Datt, B., McVicar, T. R., Van Niel, T. G., & Pearlman, J. S. (2003). Preprocessing EO-1 Hyperion hyperspectral data to support the application of agricultural indexes. *IEEE Transactions on Geoscience and Remote Sensing*, *41*(2), 1246–1259.

Driscoll, C. T., Driscoll, K. M., Roy, K. M., & Mitchell, M. J. (2003). Chemical response of lakes in the Adirondack region of New York to declines in acidic deposition. *Environmental Science and Technology*, *37*, 2036–2042.

Evans, J. (1989). Photosynthesis and nitrogen relationships in leaves of C3 plants. *Oecologia*, *78*, 9–19.

Field, C., & Mooney, H. A. (1986). The photosynthesis–nitrogen relationship in wild plants. In T. J. Givnish (Ed.), *On the economy of plant form and function* (pp. 25–55). Cambridge, UK: Cambridge Univ. Press.

Gholz, H. L., & Clark, K. L. (2002). Energy exchange across a chronosequence of slash pine forests in Florida. *Agricultural and Forest Meteorology*, *112*, 87–102.

Goulden, M. L., Munger, J. W., Fan, S. M., Daube, B. C., & Wofsy, S. C. (1996). Measurements of carbon sequestration by long-term eddy covariance: Methods and a critical evaluation of accuracy. *Global Change Biology*, *2*(3), 169–182.

Green, R. O. (2005). The AVIRIS radiometric performance model and current signal-to-noise-ratio performance. *Proceedings Of The 14th JPL Airborne Geoscience Workshop* Pasadena, CA: Jet Propulsion Laboratory.

Green, D. S., Erickson, J. E., & Kruger, E. L. (2003). Foliar morphology and canopy nitrogen as predictors of light-use efficiency in terrestrial vegetation. *Agricultural and Forest Meteorology*, *115*, 163–171.

Haxeltine, A., & Prentice, I. C. (1996). A general model for the light-use efficiency of primary production. *Functional Ecology*, *10*, 551–561.

Hollinger, D., Goltz, S., Davidson, E., Lee, J., Tu, K., & Valentine, H. (1999). Seasonal patterns and environmental control of carbon dioxide and water vapour exchange in an ecotonal boreal forest. *Global Change Biology*, *5*(8), 891–902.

Huang, Z., Turner, B. J., Dury, S. J., Wallis, I. R., & Foley, W. J. (2004). Estimating foliage nitrogen concentration from HYMAP data using continuum removal analysis. *Remote Sensing of Environment*, *93*, 18–29.

Jenkins, J., Richardson, A., Braswell, B., Ollinger, S., Hollinger, D., & Smith, M. (2007). Refining light-use efficiency calculations for a deciduous forest canopy using simultaneous tower-based carbon flux and radiometric measurements. *Agricultural and Forest Meteorology*, *143*, 64–79.

Kokaly, R. F., & Clark, R. N. (1999). Spectroscopic determination of leaf biochemistry using band-depth analysis of absorption features and stepwise multiple linear regression. *Remote Sensing of Environment*, *67*, 267–287.

Kramer, R. (1998). *Chemometric techniques for quantitative analysis.* New York: Marcel Dekker, Inc.

Kruse, F. A. (2003). Mineral mapping with AVIRIS and EO-1 Hyperion. *Proceedings Of The 12th JPL Airborne Geoscience Workshop* (pp. 149–156). Pasadena, CA: Jet Propulsion Laboratory.

Kruse, A. F. (2004). Comparison of ATREM, ACORN, and FLAASH atmospheric corrections using low-altitude AVIRIS data of Boulder. *13th JPL Airborne Geoscience Workshop*. Pasadena, CA: Jet Propulsion Laboratory.

Lee, J. J., Church, M. R., Lammers, D. A., Liegel, L., Johnson, M., Coffey, D., et al. (1989). Watershed surveys to support an assessment of the regional effects of acidic deposition on surface water chemistry. *Environmental Management*, *13*, 95–108.

Loescher, H. W., Oberbauer, S. F., Gholz, H. L., & Clark, D. B. (2003). Environmental controls on net ecosystem-level carbon exchange and productivity in a Central American tropical wet forest. *Global Change Biology*, *9*(3), 396–412.

Magill, A. H., Aber, J. D., Currie, W. S., Nadelhoffer, K. J., Martin, M. E., McDowell, W. H., et al. (2004). Ecosystem response to 15 years of chronic nitrogen additions at the Harvard Forest LTER, Massachusetts, USA. *Forest Ecology and Management*, *196*, 7–28.

Mark, H., & Workman, J. (1991). *Statistics in spectroscopy.* San Diego: Academic Press, Inc.

Martin, M. E., & Aber, J. D. (1997). High spectral resolution remote sensing of forest canopy lignin, nitrogen, and ecosystem processes. *Ecological Applications*, *4*, 431–443.

McNeil, B. E. (2006). *Spatial Variability of Foliar Nitrogen in the Adirondack Park, New York.* Syracuse University.

McNeil, B. E., Read, J. M., & Driscoll, C. T. (2005). Identifying controls on the spatial variability of foliar nitrogen in a large, complex ecosystem: The role of atmospheric nitrogen deposition in the Adirondack Park, NY. *Journal of Agricultural Meteorology*, *60*, 1157–1160.

Norris, K. H., Barnes, R. F., Moore, J. E., & Shenk, J. S. (1996). Predicting forage quality by infrared reflectance spectroscopy. *Journal of Animal Science*, *43*, 889–897.

Nowak, R. S., Ellsworth, D. S., & Smith, S. D. (2004). Functional responses of plants to elevated atmospheric CO_2: Do photosynthetic and productivity data from FACE experiments support early predictions? *New Phytologist*, *162*, 253–280.

Ollinger, S. V., & Smith, M. L. (2005). Net primary production and canopy nitrogen in a temperate forest landscape: An analysis using imaging spectroscopy, modeling, and field data. *Ecosystems*, *8*, 760–778.

Ollinger, S. V., Smith, M. L., Martin, M. E., Hallett, R. A., Aber, J. D., & Goodale, C. L. (2002). Regional variation in foliar chemistry and soil nitrogen status among forests of diverse history and composition. *Ecology*, *83*, 339–355.

Oren, R., Hsieh, C. I., Stoy, P., Albertson, J., McCarthy, H. R., Harrell, P., et al. (2006). Estimating the uncertainty in annual net ecosystem carbon exchange: Spatial variation in turbulent fluxes and sampling errors in eddy-covariance measurements. *Global Change Biology*, *12*, 883–896.

Osborne, B. G., & Fearn, T. (1986). *Near infrared spectroscopy in food analysis.* Harlow, UK: Longman Scientific and Technical Publishing Co.

Pearlman, J. S., Crawford, M., Jupp, D. L. B., & Ungar, S. (2003). Foreword to the Earth Observing 1 — Part 1, Special Issue. *IEEE Transactions on Geoscience and Remote Sensing*, *41*(6), 1147–1148.

Reich, P. B., Ellsworth, D. S., & Walters, M. B. (1998). Leaf structure (specific leaf area) modulates photosynthesis–nitrogen relations: Evidence from within and across species and functional groups. *Functional Ecology*, *12*, 948–958.

Reich, P. B., Ellsworth, D. S., Walters, M. B., Vose, J. M., Gresham, C., Volin, J. C., et al. (1999). Generality of leaf trait relationships: A test across six biomes. *Ecology*, *80*, 1955–1969.

Reich, P. B., Hobbie, S. E., Lee, T., Ellsworth, D. S., West, J. B., Tilman, D., et al. (2006). Nitrogen limitation constrains sustainability of ecosystem response to CO_2. *Nature*, *440*, 922–925.

Scott, N. A., & Binkley, D. (1997). Foliage litter quality and annual net N mineralization: Comparison across North American forest sites. *Oecologia*, *111*, 151–159.

Shenk, J. S., Westerhous, M. O., & Hoover, M. R. (1979). Analysis of forages by infrared reflectance. *Journal of Dairy Science*, *62*, 807–812.

Smith, M. L., & Martin, M. E. (2001). A plot-based method for rapid estimation of forest canopy chemistry. *Canadian Journal of Forest Research*, *31*, 549–555.

Smith, M. L., Martin, M. E., Ollinger, S. V., & Plourde, L. (2003). Analysis of hyperspectral data for estimation of temperate forest canopy nitrogen concentration: Comparison between an airborne (AVIRIS) and a spaceborne (Hyperion) sensor. *EEE Transactions on Geosciences and Remote Sensing*, *41*(6), 1332–1337.

Smith, M. L., Ollinger, S. V., Martin, M. E., Aber, J. D., Hallett, R. A., & Goodale, C. L. (2002). Direct estimation of aboveground forest productivity through hyperspectral remote sensing of canopy nitrogen. *Ecological Applications*, *12*, 1286–1302.

Townsend, P. A., Foster, J. R., Chastain, R. A., Jr., & Currie, W. S. (2003). Imaging spectroscopy and canopy nitrogen: Application to the forests of the central Appalachian Mountains using Hyperion and AVIRIS. *IEEE Transactions on Geoscience and Remote Sensing*, *41*(6), 1347–1354.

Wessman, C. A., Aber, J. D., Peterson, D. L., & Melillo, J. M. (1988). Remote sensing of canopy chemistry and nitrogen cycling in temperate forest ecosystems. *Nature*, *335*, 154–156.

Williams, P. C. (2001). Implementation of near-infrared technology. In P. Williams & K. Norris (Eds.), *Near-infrared technology in the agricultural and food industries* (pp. 145–169)., Second Edition St. Paul, Minnesota, USA: American Association of Cereal Chemists, Inc.

Williams, P. C., Preston, K. R., Norris, K. H., & Starkey, P. M. (1984). Determination of amino acids in wheat and barley by near-infrared reflectance spectroscopy. *Journal of Food Science*, *49*, 17–20.

Wofsy, S. C., Goulden, M. L., Munger, J. W., Fan, S. M., Bakwin, P. S., Daube, B. C., et al. (1993). Net exchange of CO_2 in a midlatitude forest. *Science*, *260*, 1314–1317.

Wright, I. J., Reich, P. B., Westoby, M., Ackerly, D. D., Baruch, Z., Bongers, F., et al. (2004). The worldwide leaf economics spectrum. *Nature*, *428*, 821–827.

Yin, X. (1992). Empirical relationships between temperature and nitrogen availability across North American forests. *Canadian Journal of Forest Research*, *22*, 707–712.